

Measurement of the B_s^0 Lifetime Using Semileptonic Decays

V.M. Abazov,³⁶ B. Abbott,⁷⁶ M. Abolins,⁶⁶ B.S. Acharya,²⁹ M. Adams,⁵² T. Adams,⁵⁰ M. Agelou,¹⁸ J.-L. Agram,¹⁹ S.H. Ahn,³¹ M. Ahsan,⁶⁰ G.D. Alexeev,³⁶ G. Alkhazov,⁴⁰ A. Alton,⁶⁵ G. Alverson,⁶⁴ G.A. Alves,² M. Anastasoae,³⁵ T. Andeen,⁵⁴ S. Anderson,⁴⁶ B. Andrieu,¹⁷ M.S. Anzels,⁵⁴ Y. Arnoud,¹⁴ M. Arov,⁵³ A. Askew,⁵⁰ B. Åsman,⁴¹ A.C.S. Assis Jesus,³ O. Atramentov,⁵⁸ C. Autermann,²¹ C. Avila,⁸ C. Ay,²⁴ F. Badaud,¹³ A. Baden,⁶² L. Bagby,⁵³ B. Baldin,⁵¹ D.V. Bandurin,³⁶ P. Banerjee,²⁹ S. Banerjee,²⁹ E. Barberis,⁶⁴ P. Bargassa,⁸¹ P. Baringer,⁵⁹ C. Barnes,⁴⁴ J. Barreto,² J.F. Bartlett,⁵¹ U. Bassler,¹⁷ D. Bauer,⁴⁴ A. Bean,⁵⁹ M. Begalli,³ M. Begel,⁷² C. Belanger-Champagne,⁵ A. Bellavance,⁶⁸ J.A. Benitez,⁶⁶ S.B. Beri,²⁷ G. Bernardi,¹⁷ R. Bernhard,⁴² L. Berntzon,¹⁵ I. Bertram,⁴³ M. Besançon,¹⁸ R. Beuselinck,⁴⁴ V.A. Bezzubov,³⁹ P.C. Bhat,⁵¹ V. Bhatnagar,²⁷ M. Binder,²⁵ C. Biscarat,⁴³ K.M. Black,⁶³ I. Blackler,⁴⁴ G. Blazey,⁵³ F. Blekman,⁴⁴ S. Blessing,⁵⁰ D. Bloch,¹⁹ K. Bloom,⁶⁸ U. Blumenschein,²³ A. Boehnlein,⁵¹ O. Boeriu,⁵⁶ T.A. Bolton,⁶⁰ F. Borchering,⁵¹ G. Borissov,⁴³ K. Bos,³⁴ T. Bose,⁷⁸ A. Brandt,⁷⁹ R. Brock,⁶⁶ G. Brooijmans,⁷¹ A. Bross,⁵¹ D. Brown,⁷⁹ N.J. Buchanan,⁵⁰ D. Buchholz,⁵⁴ M. Buehler,⁸² V. Buescher,²³ S. Burdin,⁵¹ S. Burke,⁴⁶ T.H. Burnett,⁸³ E. Busato,¹⁷ C.P. Buszello,⁴⁴ J.M. Butler,⁶³ S. Calvet,¹⁵ J. Cammin,⁷² S. Caron,³⁴ M.A. Carrasco-Lizarraga,³³ W. Carvalho,³ B.C.K. Casey,⁷⁸ N.M. Cason,⁵⁶ H. Castilla-Valdez,³³ S. Chakrabarti,²⁹ D. Chakraborty,⁵³ K.M. Chan,⁷² A. Chandra,⁴⁹ D. Chapin,⁷⁸ F. Charles,¹⁹ E. Cheu,⁴⁶ F. Chevallier,¹⁴ D.K. Cho,⁶³ S. Choi,³² B. Choudhary,²⁸ L. Christofek,⁵⁹ D. Claes,⁶⁸ B. Clément,¹⁹ C. Clément,⁴¹ Y. Coadou,⁵ M. Cooke,⁸¹ W.E. Cooper,⁵¹ D. Coppage,⁵⁹ M. Corcoran,⁸¹ M.-C. Cousinou,¹⁵ B. Cox,⁴⁵ S. Crépe-Renaudin,¹⁴ D. Cutts,⁷⁸ M. Ćwiok,³⁰ H. da Motta,² A. Das,⁶³ M. Das,⁶¹ B. Davies,⁴³ G. Davies,⁴⁴ G.A. Davis,⁵⁴ K. De,⁷⁹ P. de Jong,³⁴ S.J. de Jong,³⁵ E. De La Cruz-Burelo,⁶⁵ C. De Oliveira Martins,³ J.D. Degenhardt,⁶⁵ F. Déliot,¹⁸ M. Demarteau,⁵¹ R. Demina,⁷² P. Demine,¹⁸ D. Denisov,⁵¹ S.P. Denisov,³⁹ S. Desai,⁷³ H.T. Diehl,⁵¹ M. Diesburg,⁵¹ M. Doidge,⁴³ A. Dominguez,⁶⁸ H. Dong,⁷³ L.V. Dudko,³⁸ L. Dufflot,¹⁶ S.R. Dugad,²⁹ A. Duperrin,¹⁵ J. Dyer,⁶⁶ A. Dyshkant,⁵³ M. Eads,⁶⁸ D. Edmunds,⁶⁶ T. Edwards,⁴⁵ J. Ellison,⁴⁹ J. Elmsheuser,²⁵ V.D. Elvira,⁵¹ S. Eno,⁶² P. Ermolov,³⁸ J. Estrada,⁵¹ H. Evans,⁵⁵ A. Evdokimov,³⁷ V.N. Evdokimov,³⁹ S.N. Fatakia,⁶³ L. Felgioni,⁶³ A.V. Ferapontov,⁶⁰ T. Ferbel,⁷² F. Fiedler,²⁵ F. Filthaut,³⁵ W. Fisher,⁵¹ H.E. Fisk,⁵¹ I. Fleck,²³ M. Ford,⁴⁵ M. Fortner,⁵³ H. Fox,²³ S. Fu,⁵¹ S. Fuess,⁵¹ T. Gadfort,⁸³ C.F. Galea,³⁵ E. Gallas,⁵¹ E. Galyaev,⁵⁶ C. Garcia,⁷² A. Garcia-Bellido,⁸³ J. Gardner,⁵⁹ V. Gavrilov,³⁷ A. Gay,¹⁹ P. Gay,¹³ D. Gelé,¹⁹ R. Gelhaus,⁴⁹ C.E. Gerber,⁵² Y. Gershtein,⁵⁰ D. Gillberg,⁵ G. Ginther,⁷² N. Gollub,⁴¹ B. Gómez,⁸ K. Gounder,⁵¹ A. Goussiou,⁵⁶ P.D. Grannis,⁷³ H. Greenlee,⁵¹ Z.D. Greenwood,⁶¹ E.M. Gregores,⁴ G. Grenier,²⁰ Ph. Gris,¹³ J.-F. Grivaz,¹⁶ S. Grünendahl,⁵¹ M.W. Grünewald,³⁰ F. Guo,⁷³ J. Guo,⁷³ G. Gutierrez,⁵¹ P. Gutierrez,⁷⁶ A. Haas,⁷¹ N.J. Hadley,⁶² P. Haefner,²⁵ S. Hagopian,⁵⁰ J. Haley,⁶⁹ I. Hall,⁷⁶ R.E. Hall,⁴⁸ L. Han,⁷ K. Hanagaki,⁵¹ K. Harder,⁶⁰ A. Harel,⁷² R. Harrington,⁶⁴ J.M. Hauptman,⁵⁸ R. Hauser,⁶⁶ J. Hays,⁵⁴ T. Hebbeker,²¹ D. Hedin,⁵³ J.G. Hegeman,³⁴ J.M. Heinmiller,⁵² A.P. Heinson,⁴⁹ U. Heintz,⁶³ C. Hensel,⁵⁹ G. Hesketh,⁶⁴ M.D. Hildreth,⁵⁶ R. Hirosky,⁸² J.D. Hobbs,⁷³ B. Hoeneisen,¹² M. Hohlfeld,¹⁶ S.J. Hong,³¹ R. Hooper,⁷⁸ P. Houben,³⁴ Y. Hu,⁷³ V. Hynek,⁹ I. Iashvili,⁷⁰ R. Illingworth,⁵¹ A.S. Ito,⁵¹ S. Jabeen,⁶³ M. Jaffré,¹⁶ S. Jain,⁷⁶ K. Jakobs,²³ C. Jarvis,⁶² A. Jenkins,⁴⁴ R. Jesik,⁴⁴ K. Johns,⁴⁶ C. Johnson,⁷¹ M. Johnson,⁵¹ A. Jonckheere,⁵¹ P. Jonsson,⁴⁴ A. Juste,⁵¹ D. Käfer,²¹ S. Kahn,⁷⁴ E. Kajfasz,¹⁵ A.M. Kalinin,³⁶ J.M. Kalk,⁶¹ J.R. Kalk,⁶⁶ S. Kappler,²¹ D. Karmanov,³⁸ J. Kasper,⁶³ I. Katsanos,⁷¹ D. Kau,⁵⁰ R. Kaur,²⁷ R. Kehoe,⁸⁰ S. Kermiche,¹⁵ S. Kesisoglou,⁷⁸ A. Khanov,⁷⁷ A. Kharchilava,⁷⁰ Y.M. Kharzheev,³⁶ D. Khatidze,⁷¹ H. Kim,⁷⁹ T.J. Kim,³¹ M.H. Kirby,³⁵ B. Klima,⁵¹ J.M. Kohli,²⁷ J.-P. Konrath,²³ M. Kopal,⁷⁶ V.M. Korablev,³⁹ J. Kotcher,⁷⁴ B. Kothari,⁷¹ A. Koubarovsky,³⁸ A.V. Kozelov,³⁹ J. Kozminski,⁶⁶ A. Kryemadhi,⁸² S. Krzywdzinski,⁵¹ T. Kuhl,²⁴ A. Kumar,⁷⁰ S. Kunori,⁶² A. Kupco,¹¹ T. Kurča,^{20,*} J. Kvita,⁹ S. Lager,⁴¹ S. Lammers,⁷¹ G. Landsberg,⁷⁸ J. Lazoflores,⁵⁰ A.-C. Le Bihan,¹⁹ P. Lebrun,²⁰ W.M. Lee,⁵³ A. Leflat,³⁸ F. Lehner,⁴² C. Leonidopoulos,⁷¹ V. Lesne,¹³ J. Leveque,⁴⁶ P. Lewis,⁴⁴ J. Li,⁷⁹ Q.Z. Li,⁵¹ J.G.R. Lima,⁵³ D. Lincoln,⁵¹ J. Linnemann,⁶⁶ V.V. Lipaev,³⁹ R. Lipton,⁵¹ Z. Liu,⁵ L. Lobo,⁴⁴ A. Lobodenko,⁴⁰ M. Lokajicek,¹¹ A. Lounis,¹⁹ P. Love,⁴³ H.J. Lubatti,⁸³ M. Lynker,⁵⁶ A.L. Lyon,⁵¹ A.K.A. Maciel,² R.J. Madaras,⁴⁷ P. Mättig,²⁶ C. Magass,²¹ A. Magerkurth,⁶⁵ A.-M. Magnan,¹⁴ N. Makovec,¹⁶ P.K. Mal,⁵⁶ H.B. Malbouisson,³ S. Malik,⁶⁸ V.L. Malyshev,³⁶ H.S. Mao,⁶ Y. Maravin,⁶⁰ M. Martens,⁵¹ S.E.K. Mattingly,⁷⁸ R. McCarthy,⁷³ R. McCroskey,⁴⁶ D. Meder,²⁴ A. Melnitchouk,⁶⁷ A. Mendes,¹⁵ L. Mendoza,⁸ M. Merkin,³⁸ K.W. Merritt,⁵¹ A. Meyer,²¹ J. Meyer,²² M. Michaut,¹⁸ H. Miettinen,⁸¹ T. Millet,²⁰ J. Mitrevski,⁷¹ J. Molina,³ N.K. Mondal,²⁹ J. Monk,⁴⁵ R.W. Moore,⁵ T. Moulik,⁵⁹ G.S. Muanza,¹⁶ M. Mulders,⁵¹ M. Mulhearn,⁷¹

L. Mundim,³ Y.D. Mutaf,⁷³ E. Nagy,¹⁵ M. Naimuddin,²⁸ M. Narain,⁶³ N.A. Naumann,³⁵ H.A. Neal,⁶⁵ J.P. Negret,⁸ S. Nelson,⁵⁰ P. Neustroev,⁴⁰ C. Noeding,²³ A. Nomerotski,⁵¹ S.F. Novaes,⁴ T. Nunnemann,²⁵ V. O'Dell,⁵¹ D.C. O'Neil,⁵ G. Obrant,⁴⁰ V. Oguri,³ N. Oliveira,³ N. Oshima,⁵¹ R. Otec,¹⁰ G.J. Otero y Garzón,⁵² M. Owen,⁴⁵ P. Padley,⁸¹ N. Parashar,⁵⁷ S.-J. Park,⁷² S.K. Park,³¹ J. Parsons,⁷¹ R. Partridge,⁷⁸ N. Parua,⁷³ A. Patwa,⁷⁴ G. Pawloski,⁸¹ P.M. Perea,⁴⁹ E. Perez,¹⁸ K. Peters,⁴⁵ P. Pétroff,¹⁶ M. Petteni,⁴⁴ R. Piegaiia,¹ M.-A. Pleier,²² P.L.M. Podesta-Lerma,³³ V.M. Podstavkov,⁵¹ Y. Pogorelov,⁵⁶ M.-E. Pol,² A. Pompoš,⁷⁶ B.G. Pope,⁶⁶ A.V. Popov,³⁹ W.L. Prado da Silva,³ H.B. Prosper,⁵⁰ S. Protopopescu,⁷⁴ J. Qian,⁶⁵ A. Quadt,²² B. Quinn,⁶⁷ K.J. Rani,²⁹ K. Ranjan,²⁸ P.A. Rapidis,⁵¹ P.N. Ratoff,⁴³ P. Renkel,⁸⁰ S. Reucroft,⁶⁴ M. Rijssenbeek,⁷³ I. Ripp-Baudot,¹⁹ F. Rizatdinova,⁷⁷ S. Robinson,⁴⁴ R.F. Rodrigues,³ C. Royon,¹⁸ P. Rubinov,⁵¹ R. Ruchti,⁵⁶ V.I. Rud,³⁸ G. Sajot,¹⁴ A. Sánchez-Hernández,³³ M.P. Sanders,⁶² A. Santoro,³ G. Savage,⁵¹ L. Sawyer,⁶¹ T. Scanlon,⁴⁴ D. Schaile,²⁵ R.D. Schamberger,⁷³ Y. Scheglov,⁴⁰ H. Schellman,⁵⁴ P. Schieferdecker,²⁵ C. Schmitt,²⁶ C. Schwanenberger,⁴⁵ A. Schwartzman,⁶⁹ R. Schwienhorst,⁶⁶ S. Sengupta,⁵⁰ H. Severini,⁷⁶ E. Shabalina,⁵² M. Shamim,⁶⁰ V. Shary,¹⁸ A.A. Shchukin,³⁹ W.D. Shephard,⁵⁶ R.K. Shivpuri,²⁸ D. Shpakov,⁶⁴ V. Siccardi,¹⁹ R.A. Sidwell,⁶⁰ V. Simak,¹⁰ V. Sirotenko,⁵¹ P. Skubic,⁷⁶ P. Slattery,⁷² R.P. Smith,⁵¹ G.R. Snow,⁶⁸ J. Snow,⁷⁵ S. Snyder,⁷⁴ S. Söldner-Rembold,⁴⁵ X. Song,⁵³ L. Sonnenschein,¹⁷ A. Sopczak,⁴³ M. Sosebee,⁷⁹ K. Soustruznik,⁹ M. Souza,² B. Spurlock,⁷⁹ J. Stark,¹⁴ J. Steele,⁶¹ K. Stevenson,⁵⁵ V. Stolin,³⁷ A. Stone,⁵² D.A. Stoyanova,³⁹ J. Strandberg,⁴¹ M.A. Strang,⁷⁰ M. Strauss,⁷⁶ R. Ströhmer,²⁵ D. Strom,⁵⁴ M. Strovink,⁴⁷ L. Stutte,⁵¹ S. Sumowidagdo,⁵⁰ A. Sznajder,³ M. Talby,¹⁵ P. Tamburello,⁴⁶ W. Taylor,⁵ P. Telford,⁴⁵ J. Temple,⁴⁶ B. Tiller,²⁵ M. Titov,²³ V.V. Tokmenin,³⁶ M. Tomoto,⁵¹ T. Toole,⁶² I. Torchiani,²³ S. Towers,⁴³ T. Trefzger,²⁴ S. Trincz-Duvoid,¹⁷ D. Tsybychev,⁷³ B. Tuchming,¹⁸ C. Tully,⁶⁹ A.S. Turcot,⁴⁵ P.M. Tuts,⁷¹ R. Unalan,⁶⁶ L. Uvarov,⁴⁰ S. Uvarov,⁴⁰ S. Uzunyan,⁵³ B. Vachon,⁵ P.J. van den Berg,³⁴ R. Van Kooten,⁵⁵ W.M. van Leeuwen,³⁴ N. Varelas,⁵² E.W. Varnes,⁴⁶ A. Vartapetian,⁷⁹ I.A. Vasilyev,³⁹ M. Vaupel,²⁶ P. Verdier,²⁰ L.S. Vertogradov,³⁶ M. Verzocchi,⁵¹ F. Villeneuve-Seguiet,⁴⁴ P. Vint,⁴⁴ J.-R. Vlimant,¹⁷ E. Von Toerne,⁶⁰ M. Voutilainen,^{68,†} M. Vreeswijk,³⁴ H.D. Wahl,⁵⁰ L. Wang,⁶² J. Warchol,⁵⁶ G. Watts,⁸³ M. Wayne,⁵⁶ M. Weber,⁵¹ H. Weerts,⁶⁶ N. Wermes,²² M. Wetstein,⁶² A. White,⁷⁹ D. Wicke,²⁶ G.W. Wilson,⁵⁹ S.J. Wimpenny,⁴⁹ M. Wobisch,⁵¹ J. Womersley,⁵¹ D.R. Wood,⁶⁴ T.R. Wyatt,⁴⁵ Y. Xie,⁷⁸ N. Xuan,⁵⁶ S. Yacoob,⁵⁴ R. Yamada,⁵¹ M. Yan,⁶² T. Yasuda,⁵¹ Y.A. Yatsunenko,³⁶ K. Yip,⁷⁴ H.D. Yoo,⁷⁸ S.W. Youn,⁵⁴ C. Yu,¹⁴ J. Yu,⁷⁹ A. Yurkewicz,⁷³ A. Zatserklyaniy,⁵³ C. Zeitnitz,²⁶ D. Zhang,⁵¹ T. Zhao,⁸³ Z. Zhao,⁶⁵ B. Zhou,⁶⁵ J. Zhu,⁷³ M. Zielinski,⁷² D. Zieminska,⁵⁵ A. Zieminski,⁵⁵ V. Zutshi,⁵³ and E.G. Zverev³⁸
(DØ Collaboration)

¹ Universidad de Buenos Aires, Buenos Aires, Argentina

² LAFEX, Centro Brasileiro de Pesquisas Físicas, Rio de Janeiro, Brazil

³ Universidade do Estado do Rio de Janeiro, Rio de Janeiro, Brazil

⁴ Instituto de Física Teórica, Universidade Estadual Paulista, São Paulo, Brazil

⁵ University of Alberta, Edmonton, Alberta, Canada, Simon Fraser University, Burnaby, British Columbia, Canada, York University, Toronto, Ontario, Canada, and McGill University, Montreal, Quebec, Canada

⁶ Institute of High Energy Physics, Beijing, People's Republic of China

⁷ University of Science and Technology of China, Hefei, People's Republic of China

⁸ Universidad de los Andes, Bogotá, Colombia

⁹ Center for Particle Physics, Charles University, Prague, Czech Republic

¹⁰ Czech Technical University, Prague, Czech Republic

¹¹ Center for Particle Physics, Institute of Physics, Academy of Sciences of the Czech Republic, Prague, Czech Republic

¹² Universidad San Francisco de Quito, Quito, Ecuador

¹³ Laboratoire de Physique Corpusculaire, IN2P3-CNRS, Université Blaise Pascal, Clermont-Ferrand, France

¹⁴ Laboratoire de Physique Subatomique et de Cosmologie, IN2P3-CNRS, Université de Grenoble 1, Grenoble, France

¹⁵ CPPM, IN2P3-CNRS, Université de la Méditerranée, Marseille, France

¹⁶ IN2P3-CNRS, Laboratoire de l'Accélérateur Linéaire, Orsay, France

¹⁷ LPNHE, IN2P3-CNRS, Universités Paris VI and VII, Paris, France

¹⁸ DAPNIA/Service de Physique des Particules, CEA, Saclay, France

¹⁹ IReS, IN2P3-CNRS, Université Louis Pasteur, Strasbourg, France, and Université de Haute Alsace, Mulhouse, France

²⁰ Institut de Physique Nucléaire de Lyon, IN2P3-CNRS, Université Claude Bernard, Villeurbanne, France

²¹ III. Physikalisches Institut A, RWTH Aachen, Aachen, Germany

²² Physikalisches Institut, Universität Bonn, Bonn, Germany

²³ Physikalisches Institut, Universität Freiburg, Freiburg, Germany

²⁴ Institut für Physik, Universität Mainz, Mainz, Germany

²⁵ Ludwig-Maximilians-Universität München, München, Germany

²⁶ Fachbereich Physik, University of Wuppertal, Wuppertal, Germany

²⁷ Panjab University, Chandigarh, India

- ²⁸ Delhi University, Delhi, India
- ²⁹ Tata Institute of Fundamental Research, Mumbai, India
- ³⁰ University College Dublin, Dublin, Ireland
- ³¹ Korea Detector Laboratory, Korea University, Seoul, Korea
- ³² SungKyunKwan University, Suwon, Korea
- ³³ CINVESTAV, Mexico City, Mexico
- ³⁴ FOM-Institute NIKHEF and University of Amsterdam/NIKHEF, Amsterdam, The Netherlands
- ³⁵ Radboud University Nijmegen/NIKHEF, Nijmegen, The Netherlands
- ³⁶ Joint Institute for Nuclear Research, Dubna, Russia
- ³⁷ Institute for Theoretical and Experimental Physics, Moscow, Russia
- ³⁸ Moscow State University, Moscow, Russia
- ³⁹ Institute for High Energy Physics, Protvino, Russia
- ⁴⁰ Petersburg Nuclear Physics Institute, St. Petersburg, Russia
- ⁴¹ Lund University, Lund, Sweden, Royal Institute of Technology and Stockholm University, Stockholm, Sweden, and Uppsala University, Uppsala, Sweden
- ⁴² Physik Institut der Universität Zürich, Zürich, Switzerland
- ⁴³ Lancaster University, Lancaster, United Kingdom
- ⁴⁴ Imperial College, London, United Kingdom
- ⁴⁵ University of Manchester, Manchester, United Kingdom
- ⁴⁶ University of Arizona, Tucson, Arizona 85721, USA
- ⁴⁷ Lawrence Berkeley National Laboratory and University of California, Berkeley, California 94720, USA
- ⁴⁸ California State University, Fresno, California 93740, USA
- ⁴⁹ University of California, Riverside, California 92521, USA
- ⁵⁰ Florida State University, Tallahassee, Florida 32306, USA
- ⁵¹ Fermi National Accelerator Laboratory, Batavia, Illinois 60510, USA
- ⁵² University of Illinois at Chicago, Chicago, Illinois 60607, USA
- ⁵³ Northern Illinois University, DeKalb, Illinois 60115, USA
- ⁵⁴ Northwestern University, Evanston, Illinois 60208, USA
- ⁵⁵ Indiana University, Bloomington, Indiana 47405, USA
- ⁵⁶ University of Notre Dame, Notre Dame, Indiana 46556, USA
- ⁵⁷ Purdue University Calumet, Hammond, Indiana 46323, USA
- ⁵⁸ Iowa State University, Ames, Iowa 50011, USA
- ⁵⁹ University of Kansas, Lawrence, Kansas 66045, USA
- ⁶⁰ Kansas State University, Manhattan, Kansas 66506, USA
- ⁶¹ Louisiana Tech University, Ruston, Louisiana 71272, USA
- ⁶² University of Maryland, College Park, Maryland 20742, USA
- ⁶³ Boston University, Boston, Massachusetts 02215, USA
- ⁶⁴ Northeastern University, Boston, Massachusetts 02115, USA
- ⁶⁵ University of Michigan, Ann Arbor, Michigan 48109, USA
- ⁶⁶ Michigan State University, East Lansing, Michigan 48824, USA
- ⁶⁷ University of Mississippi, University, Mississippi 38677, USA
- ⁶⁸ University of Nebraska, Lincoln, Nebraska 68588, USA
- ⁶⁹ Princeton University, Princeton, New Jersey 08544, USA
- ⁷⁰ State University of New York, Buffalo, New York 14260, USA
- ⁷¹ Columbia University, New York, New York 10027, USA
- ⁷² University of Rochester, Rochester, New York 14627, USA
- ⁷³ State University of New York, Stony Brook, New York 11794, USA
- ⁷⁴ Brookhaven National Laboratory, Upton, New York 11973, USA
- ⁷⁵ Langston University, Langston, Oklahoma 73050, USA
- ⁷⁶ University of Oklahoma, Norman, Oklahoma 73019, USA
- ⁷⁷ Oklahoma State University, Stillwater, Oklahoma 74078, USA
- ⁷⁸ Brown University, Providence, Rhode Island 02912, USA
- ⁷⁹ University of Texas, Arlington, Texas 76019, USA
- ⁸⁰ Southern Methodist University, Dallas, Texas 75275, USA
- ⁸¹ Rice University, Houston, Texas 77005, USA
- ⁸² University of Virginia, Charlottesville, Virginia 22901, USA
- ⁸³ University of Washington, Seattle, Washington 98195, USA

(Dated:)

We report a measurement of the B_s^0 lifetime in the semileptonic decay channel $B_s^0 \rightarrow D_s^- \mu^+ \nu X$ (and its charge conjugate), using approximately 0.4 fb^{-1} of data collected with the D0 detector during 2002–2004. Using 5176 reconstructed $D_s^- \mu^+$ signal events, we have measured the B_s^0 lifetime to be $\tau(B_s^0) = 1.398 \pm 0.044 \text{ (stat)}_{-0.025}^{+0.028} \text{ (syst)} \text{ ps}$. This is the most precise measurement of the B_s^0

lifetime to date.

PACS numbers: 13.25.Hw,14.40.Nd

Measurements of the lifetimes of different b hadrons allow tests of the mechanism of heavy hadron decay. The spectator model predicts that all hadrons with the same heavy flavor content have identical lifetimes. However, observed charm and bottom hadron lifetimes suggest that non-spectator effects, such as interference between contributing amplitudes, are not negligible in heavy hadron decays. This implies that a mechanism beyond the simple spectator model is required. An effective theory called the Heavy Quark Expansion (HQE) [1] includes such effects and predicts lifetime differences among the different bottom hadrons. In particular, a difference of the order of 1% is predicted between B^0 and B_s^0 mesons. The measurement of the flavor-specific B_s^0 lifetime using semileptonic decays is also useful in determining the decay width difference between the light and heavy mass eigenstates of the B_s^0 meson, which is an equal mixture of CP eigenstates that correspond to mass eigenstates in the absence of CP violation in the B_s^0 system.

In this Letter, we present a high-statistics measurement of the B_s^0 lifetime, using a large sample of semileptonic B_s^0 decays collected in $p\bar{p}$ collisions at $\sqrt{s} = 1.96$ TeV with the D0 detector at the Fermilab Tevatron Collider in 2002 – 2004. The data correspond to approximately 0.4 fb^{-1} of integrated luminosity. B_s^0 mesons were identified through their semileptonic decay $B_s^0 \rightarrow D_s^- \mu^+ \nu X$ [13], where the D_s^- meson decays via $D_s^- \rightarrow \phi \pi^-$, followed by $\phi \rightarrow K^+ K^-$.

The D0 detector is described in detail elsewhere [2]. The detector components most important to this analysis are the central tracking and muon systems. The D0 central-tracking system consists of a silicon microstrip tracker (SMT) and a central fiber tracker (CFT), both located within a 2 T superconducting solenoidal magnet, with designs optimized for tracking and vertexing at pseudorapidities $|\eta| < 3$ and $|\eta| < 2.5$, respectively (where $\eta = -\ln[\tan(\theta/2)]$). A liquid-argon and uranium calorimeter has a central section covering pseudorapidities up to ≈ 1.1 , and two end calorimeters that extend the coverage to $|\eta| \approx 4.2$ [3]. The muon system is located outside the calorimeters and has pseudorapidity coverage $|\eta| < 2$. It consists of a layer of tracking detectors and scintillation trigger counters in front of 1.8 T toroids, followed by two similar layers after the toroids [4].

Events with semileptonic B -meson decays were selected using inclusive single-muon triggers in a three-level trigger system. The triggers used did not impose any impact parameter criterion and were shown to not bias the lifetime measurement. Off-line, muons were identified by extrapolation of the muon track segments, formed by the hits in the muon system, to the tracks found in the central tracking system. Each muon was required to have

a momentum $p > 3 \text{ GeV}/c$ and a transverse momentum $p_T > 2 \text{ GeV}/c$.

The primary vertex of each $p\bar{p}$ interaction was defined by all available well-reconstructed tracks [5] and constrained by the mean beam-spot position. The latter was updated every few hours. The resolution of the reconstructed primary vertex was typically $20 \mu\text{m}$ in the transverse plane and $40 \mu\text{m}$ in the beam direction.

To reconstruct $D_s^- \rightarrow \phi \pi^-$ decays, tracks with $p_T > 1.0 \text{ GeV}/c$ were assigned the kaon mass and oppositely charged pairs were combined to form a ϕ candidate. Each ϕ candidate was required to have a mass in the range $1.008 - 1.032 \text{ GeV}/c^2$, compatible with the reconstructed ϕ mass at D0. The ϕ candidate was then combined with another track of $p_T > 0.7 \text{ GeV}/c$. For the “right-sign” combinations, we required the charge of the track to be opposite to that of the muon and assigned the pion mass to this track. All selected tracks were required to have at least one SMT hit and one CFT hit. The three tracks selected were combined to form a common vertex (the D_s^- vertex) with a confidence level greater than 0.1%. The D_s^- candidate was required to have $p_T > 3.5 \text{ GeV}/c$.

The secondary vertex, where the B_s^0 decays to a muon and a D_s^- meson, was obtained by finding the intersection of the trajectory of the muon track and the flight path of the D_s^- candidate. The confidence level of that vertex had to be greater than 0.01%. The reconstructed D_s^- decay vertex was required to be displaced from the primary vertex in the direction of the D_s^- momentum.

The helicity angle, Φ , defined as the angle between the directions of the K^- and D_s^- in the ϕ rest frame, has a distribution proportional to $\cos^2 \Phi$. A cut of $|\cos \Phi| > 0.4$ was applied to further reduce combinatorial background, which was found to have a flat distribution. In order to suppress the physics background originating from $D^{(*)}D^{(*)}$ processes [14], we required that the transverse momentum of the muon with respect to the D_s^- meson, p_{Trel} , exceed $2 \text{ GeV}/c$. The $D_s^- \mu^+$ invariant mass was also restricted to $3.4 - 5.0 \text{ GeV}/c^2$, to be consistent with a B -meson candidate. Since the number of tracks near the B_s^0 candidate tends to be small, we required the isolation $\mathcal{I} = p^{tot}(\mu^+ D_s^-)/(p^{tot}(\mu^+ D_s^-) + \sum p_i^{tot}) > 0.65$, where the sum $\sum p_i^{tot}$ was taken over all charged particles in the cone $\sqrt{(\Delta\phi)^2 + (\Delta\eta)^2} < 0.5$, with $\Delta\phi$ and $\Delta\eta$ being the azimuthal angle and the pseudorapidity with respect to the $(\mu^+ D_s^-)$ direction. The muon, kaon, and pion tracks were not included in the sum.

The lifetime of the B_s^0 , τ , is related to the decay length in the transverse plane, L_{xy} , by $L_{xy} = c\tau p_T/m$, where p_T is the transverse momentum of the B_s^0 and m is its invariant mass. L_{xy} is defined as the displacement of the B_s^0 vertex from the primary vertex pro-

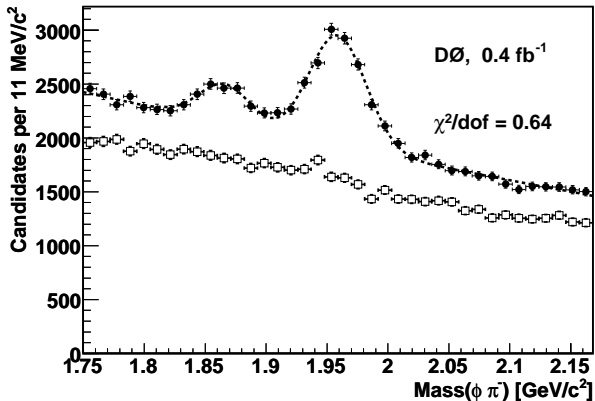


FIG. 1: The mass distribution of $\phi\pi^-$ candidates. Points with errors bars show the “right-sign” $D_s^- \mu^+$ combinations, and the open squares show the corresponding “wrong-sign” distribution. The dashed curve represents the result of the fit to the “right-sign” combinations. The two peaks are associated with the D^- and D_s^- mesons, respectively.

jected onto the transverse momentum of the $D_s^- \mu^+$ system. Since the B_s^0 meson is not fully reconstructed, $p_T(B_s^0)$ is estimated by $p_T(D_s^- \mu^+)/K$, where the correction factor, $K = p_T(D_s^- \mu^+)/p_T(B_s^0)$ is determined using Monte Carlo (MC) methods. The quantity used to extract the B_s^0 lifetime is called the pseudo-proper decay length (PPDL). The correction factor K was applied statistically when extracting $c\tau(B_s^0)$ from the PPDL in the lifetime fit.

In the cases with more than one B_s^0 candidate per event, we chose the one with the highest vertex confidence level. We also required the PPDL uncertainty to be less than $500 \mu\text{m}$. The resulting invariant mass distribution of the D_s^- candidates is shown in Fig. 1. The distribution for “right-sign” $D_s^- \mu^+$ candidates was fitted using a Gaussian, to describe the signal, and a second-order polynomial, to describe the combinatorial background. A second Gaussian was included for the Cabibbo-suppressed $D^- \rightarrow \phi\pi^-$ decay. The best fit result is shown in the same figure. The fit yields a signal of 5176 ± 242 (stat) ± 314 (syst) D_s^- candidates and a mass of $1958.8 \pm 0.9 \text{ MeV}/c^2$. The width of the D_s^- Gaussian is $22.6 \pm 1.0 \text{ MeV}/c^2$. The systematic uncertainty comes from the fit. For the D^- meson, the fit yields 1551 events. Figure 1 also shows the invariant mass distribution of the “wrong-sign” candidates. The observed shift in the D_s^- mass is consistent with known issues associated with the calibration of the D0 track momenta. The contribution to the mass region from reflected states was found to be negligible. Studies confirmed that this mass shift introduces no significant residual bias in the lifetime determination.

MC samples were generated using PYTHIA [6] for the production and hadronization phase, and EVTGEN [7] for decaying the b and c hadrons. Branching ratios from

the PDG have been used when available. Detector acceptance and smearing were taken into account using the full D0 detector simulation based on GEANT [8]. Generated MC signal samples include contributions from $D_s^- \mu^+ \nu$, $D_s^{*-} \mu^+ \nu$, $D_{s0}^{*-} \mu^+ \nu$, $D_{s1}^{*-} \mu^+ \nu$, and $D_s^{(*)-} \tau^+ \nu$.

Apart from the background due to combinatorial processes such as a prompt muon and an identified D_s^- meson, there are several real physics processes that produce a muon and a D_s^- meson, where neither comes from the semileptonic decay of the B_s^0 meson. These “right-sign” $D_s^- \mu^+$ combinations are included in the signal sample and are defined as “physics backgrounds.” Prompt D_s^- mesons from $c\bar{c}$ production at the interaction point can combine with high- p_T muons generated either via direct production or in charm decays. These $c\bar{c}$ background events are expected to have very short lifetimes and thus could introduce a significant bias in the B_s^0 lifetime measurement. Backgrounds that originate from \bar{B} mesons and provide the $D_s^- \mu^+$ final state, but not via the semileptonic decay $B_s^0 \rightarrow D_s^- \mu^+ \nu X$, are called non- B_s^0 backgrounds. This kind of background is expected to have a relatively long lifetime, thus its effect on the B_s^0 lifetime fit is smaller than that of the charm background. There are three sources of such events: $\bar{B}^0 \rightarrow D_s^{(*)-} D^{(*)+} X$, $B^- \rightarrow D_s^{(*)-} \bar{D}^{(*)0} X$, and $\bar{B}_s^0 \rightarrow D_s^{(*)-} D^{(*)+} X$, where the charm meson accompanying the $D_s^{(*)-}$, which decays to $\phi\pi^-$, decays semileptonically. The momentum of the muon coming from the decay of the $D^{(*)}$ is softer than that for the signal, since it comes from the decay of a secondary charm hadron. This implies that the contribution of these modes to the signal sample is reduced by the kinematic cuts. We found the fractional contribution of the backgrounds to the signal region to be $(10.0 \pm 7.0)\%$ for $c\bar{c}$ background and $(11.3^{+5.3}_{-3.6})\%$ for non- B_s^0 backgrounds.

The lifetime of the B_s^0 was found using a fit to the PPDL distribution. We defined a signal sample using the D_s^- mass distribution in the region from $1913.6 \text{ MeV}/c^2$ to $2004.0 \text{ MeV}/c^2$, corresponding to $\pm 2\sigma$ from the fitted mean mass. The PPDL distribution of the combinatorial background events contained in the signal sample was defined using “right-sign” events from the D_s^- sidebands ($1755.3 - 1800.5 \text{ MeV}/c^2$ and $2117.1 - 2162.3 \text{ MeV}/c^2$) and “wrong-sign” events between 1755.3 and $2162.3 \text{ MeV}/c^2$. The combinatorial background due to random track combinations was modeled by the sideband sample events. This assumption is supported by the mass distribution of the “wrong-sign” combinations where no enhancement is visible in the D_s^- mass region.

The PPDL distribution obtained from the signal sample was fitted using an unbinned maximum log-likelihood method. Both the B_s^0 lifetime and the background shape were determined in a simultaneous fit to the signal and background samples. The likelihood function \mathcal{L} is given by

$$\mathcal{L} = \mathcal{C}_{sig} \prod_i^{N_S} [f_{sig} \mathcal{F}_{sig}^i + (1 - f_{sig}) \mathcal{F}_{bck}^i] \prod_j^{N_B} \mathcal{F}_{bck}^j, \quad (1)$$

where N_S , N_B are the number of events in the signal and background samples and f_{sig} is the ratio of D_s^- signal events obtained from the D_s^- mass distribution fit to the total number of events in the signal sample. To constrain f_{sig} , we factored in an additional likelihood term using the number of D_s^- signal events observed from the invariant mass distribution, and its uncertainty, \mathcal{C}_{sig} .

Since the current world average width difference between the light and heavy mass eigenstates ($\Delta\Gamma_s$) of the B_s^0 system is small [10] compared with the current precision of the data, we used for the signal probability distribution function (PDF), \mathcal{F}_{sig}^i , a normalized single exponential decay function convoluted with a Gaussian resolution function. The K -factor correction was also convoluted with the exponential decay function. Since a priori, we do not know the decay length uncertainty, which we estimated on an event-by-event basis, an overall global scale factor, s , was introduced as a free parameter in the B_s^0 lifetime fit. The events from non- B_s^0 background were taken into account in the fit by including similar PDFs to those in the signal but using fixed parameters according to the world-average values [9]. A different K -factor distribution was also used for each process. To take into account the $c\bar{c}$ background, we used a Gaussian distribution with fixed parameters. These contributions were evaluated and parametrized using MC methods following a similar procedure as for the signal evaluation.

The combinatorial background sample, \mathcal{F}_{bck}^i , was parametrized using a Gaussian distribution function for the resolution plus several exponential decays: two for the negative values in the PDDL distribution (one short and one long component) and two for the positive values of the distribution.

Figure 2 shows the PDDL distribution of the $D_s^- \mu^+$ signal sample with the fit result superimposed (dashed curve). The dotted curve represents the sum of the background probability function over the events in the signal sample. The B_s^0 signal is represented by the filled area.

To test the resolutions, pulls, fitting, and selection criteria, we performed detailed studies using MC samples and found no significant bias in our analysis procedure. In order to study the stability of the B_s^0 lifetime measurement, we split the data sample into two parts according to different kinematic and geometric parameters, compared the fitted results, and found the lifetimes consistent within their uncertainties. We also varied the selection criteria and mass fit ranges, and did not observe any significant shifts. We performed an extensive study of our fitting procedure, looking for any possible bias using MC ensembles with statistics of the size of our dataset and distributions as those in data. These samples were

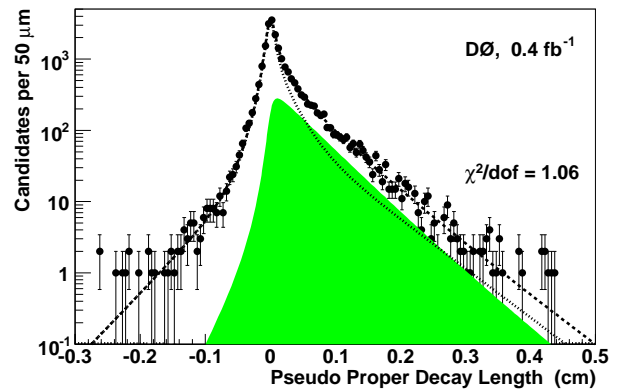


FIG. 2: Pseudo-proper decay length distribution for $D_s^- \mu^+$ candidates with the result of the fit superimposed as the dashed curve. The dotted curve represents the combinatorial background and the filled area represents the B_s^0 signal.

fitted, and the mean and width of the distributions of extracted parameters were found to be consistent with the fits to data. One final check of the procedure involved performing a similar lifetime fit to a control sample defined by the Cabibbo-suppressed decay $D^- \rightarrow \phi \pi^-$, (see Fig. 1). We found that 89.1% of the sample comes from $B^0 \rightarrow D^- \mu^+ X$, and the B^0 lifetime to be 1.541 ± 0.093 ps, where the uncertainty is statistical only. This result is in good agreement with the world average B^0 lifetime [9, 10].

We considered and evaluated various sources of systematic uncertainties. The major contributions come from the determination of the combinatorial background, the model for the resolution, and the physics background. To determine the systematics due to the uncertainty on the combinatorial background, we tested other assumptions on the background samples: we used just the events in the sidebands, just the events in the wrong-sign combinations, and removed either the right sideband or the left sideband samples. We also modified the definitions of those samples, changing the mass window sizes and positions. The largest difference in $c\tau$ observed in these variations of background modeling was $4.3 \mu\text{m}$, which was taken to be the systematic uncertainty due to this source. The effect of uncertainty in the resolution of the decay length was studied using an alternative global scale factor, s . We repeated the lifetime fit with fixed values of s obtained from MC samples and from a different lifetime analysis [11]. Using a variation of the resolution scale by a factor of two beyond these bounds, we found a $3.7 \mu\text{m}$ variation in $c\tau$. The uncertainty from the physics background was evaluated by varying the branching fractions of the different processes as well as the shapes of the lifetime templates, as given by their known lifetime values [9]. The variations were within one standard deviation in each case. Assuming no correlation between

them, we added the effects of all the variations in quadrature and found a total contribution of $^{+2.9}_{-4.2} \mu\text{m}$. Using a similar procedure, we evaluated the uncertainty coming from the determination of the $c\bar{c}$ background and found a difference of $^{+2.3}_{-0.8} \mu\text{m}$.

To evaluate the uncertainty associated with the K factor determination, we modified the kinematics of the event using a different decay model, a different p_T spectrum for the b quark, and a different p_T spectrum for the muon. We also varied the amount of each component, according to their uncertainty, of the $B_s^0 \rightarrow D_s^- \mu^+ X$ signal. In each case, the K factor was re-evaluated and the fit repeated. We added all K factor variation effects in quadrature and found a total uncertainty of $^{+3.6}_{-2.1} \mu\text{m}$.

There are two requirements in our selection method that could potentially change the final result by altering the shape of the PPDL distribution: $p_{Trel} > 2 \text{ GeV}/c$ and the positive displacement from the primary vertex of the reconstructed D_s^- decay vertex. Using MC methods, we evaluated their effects by removing them one at a time. The largest variation observed was $^{+3.0}_{-0.3} \mu\text{m}$, and the selection efficiency is flat as a function of proper decay time. The effect of a possible misalignment of the SMT system was tested in Ref. [11]. We repeated the study using MC signal samples and observed the same shift of $c\tau = 2 \mu\text{m}$, which was taken as a systematic uncertainty due to possible misalignment. The total systematic uncertainty from all of these sources added in quadrature is $^{+8.4}_{-7.6} \mu\text{m}$.

In summary, using an integrated luminosity of approximately 0.4 fb^{-1} , we have measured the B_s^0 lifetime in the decay channel $D_s^- \mu^+ \nu X$ to be $\tau(B_s^0) = 1.398 \pm 0.044$ (stat) $^{+0.028}_{-0.025}$ (syst) ps. Note that this measurement takes $\Delta\Gamma_s$ equal to zero. The extraction of the average lifetime $\bar{\tau}_s$ for $\Delta\Gamma_s \neq 0$ is straight forward [10]. The result is in good agreement with previous experiments as well as the current world average value for all flavor-specific decays, $\tau(B_s^0) = 1.442 \pm 0.066$ ps [10, 12]. Our B_s^0 lifetime measurement is the most precise to date and exceeds the precision of the current world average measurement $\tau(B_s^0)_{PDG} = 1.461 \pm 0.057$ ps [9], where semileptonic and hadronic decays were combined. This measurement is approximately 2.5σ away from the B^0 lifetime, more than the 1% predicted by HQE.

We thank the staffs at Fermilab and collaborating institutions, and acknowledge support from the DOE and NSF (USA); CEA and CNRS/IN2P3 (France); FASI, Rosatom and RFBR (Russia); CAPES, CNPq, FAPERJ, FAPESP and FUNDUNESP (Brazil); DAE and DST (India); Colciencias (Colombia); CONACyT (Mexico); KRF and KOSEF (Korea); CONICET and UBACyT (Argentina); FOM (The Netherlands); PPARC (United Kingdom); MSMT (Czech Republic); CRC Program, CFI, NSERC and WestGrid Project (Canada); BMBF and DFG (Germany); SFI (Ireland); The Swedish Research Council (Sweden); Research Corporation; Alexander von Humboldt Foundation; and the Marie Curie Program.

-
- [*] On leave from IEP SAS Kosice, Slovakia.
 - [†] Visitor from Helsinki Institute of Physics, Helsinki, Finland.
 - [1] I.I. Bigi *et al.*, in “ B decays,” 2nd edition, edited by S. Stone (World Scientific, Singapore, 1994).
 - [2] V. Abazov *et al.*, Nucl. Instrum. Meth. A **565**, 463 (2006).
 - [3] S. Abachi *et al.*, Nucl. Instrum. Methods Phys. Res. A **338**, 185 (1994).
 - [4] V. Abazov *et al.*, Nucl. Instrum. Methods Phys. Res. A **552**, 372 (2005).
 - [5] J. Abdallah *et al.*, Eur. Phys. J. C **32**, 185, (2004).
 - [6] T. Sjöstrand *et al.*, Comp. Phys. Commun. **135**, 238 (2001), v6.2.
 - [7] D. J. Lange, Nucl. Instrum. Methods Phys. Res. A **462**, 152 (2001), v00-11-07.
 - [8] R. Brun *et al.*, CERN Report No. DD/EE/84-1, 1984.
 - [9] Particle Data Group, S. Eidelman *et al.*, Phys. Lett. B **592**, 1 (2004).
 - [10] K. Anikeev *et al.* (Heavy Flavor Averaging Group), hep-ex/0505100.
 - [11] V. Abazov *et al.*, Phys. Rev. Lett. **94**, 042001 (2005).
 - [12] D. Buskulic *et al.*, Phys. Lett. B **377**, 205 (1996); K. Ackerstaff *et al.*, Phys. Lett. B **426**, 161 (1998); F. Abe *et al.*, Phys. Rev. D **59**, 032004 (1999); P. Abreu *et al.*, Eur. Phys. J. C **16**, 555 (2000).
 - [13] Unless otherwise stated, charge-conjugate states are implied.
 - [14] $D^{(*)}$ denotes either D , D^* or D^{**} .